

ENSK-ph/97-04
cond-mat/9802271

Exact four-spinon dynamical correlation function

A. Abada¹, A.H. Bougourzi², S. Seba¹ and B. Si-Lakhal¹ *

¹ Département de Physique, École Normale Supérieure

PB 92 Vieux-Kouba, 16050 Alger, Algeria.

² Department of Mathematics and Physics, Concordia University
7141 Sherbrooke St. West, Montreal, Québec H4B 1R6, Canada.

Abstract

We discuss some properties of the exact four-spinon dynamical correlation function in the antiferromagnetic spin 1/2 XXX -model the expression of which we derived recently. We show that the region in which it is not identically zero is different from and larger than the spin-wave continuum. We discuss its behavior as a function of the neutron momentum transfer k for fixed values of the neutron energy ω and compare it to the one corresponding to the exact two-spinon dynamical correlation function. We show that the overall shapes are quite similar but there are differences that we discuss. Particular is the fact that the symmetry about the axis $k = \pi$ present in the two-spinon case seems to be lost in the four-spinon one. We finish with concluding remarks.

ENSK-ph/97-04

February 1998

Typeset using REVTEX

*e-mail: enskppps@ist.cerist.dz, bougourz@alcor.concordia.ca.

I. INTRODUCTION

Quantum spin chains have been the subject of intensive study during the past seven decades [1]. Experimentally, their properties are investigated via inelastic neutron scattering on (anti)ferromagnetic quasi one-dimensional compounds [2]. One important quantity that holds much of the information related to such compounds is the dynamical correlation function (DCF) S of two local spin operators. Indeed, the neutron scattering intensity is directly proportional to it, see for example [2].

An important feature of these chains is that some of them, like the Heisenberg model, are amenable to exact theoretical treatment while still describing nontrivial interactions [1], see also [3]. This is because they incorporate in them a rich mathematical structure: the quantum affine algebra. The early work on such models consisted in determining exactly their static thermodynamic properties, see [1], whereas, more recently, a fuller exploitation of the quantum symmetry using bosonization techniques has allowed for a more systematic description of their dynamical properties [4]. A systematic account of this work is given in [5].

However, one aspect of these new techniques is that the exact correlation functions are usually obtained in the form of quite complicated contour integrals and this renders their manipulation somewhat cumbersome. But on the other hand, before this exact treatment, the approach to these dynamical quantities was only approximate. Indeed, if one considers for instance the DCF in the antiferromagnetic Heisenberg model, the focus has for a long time been only on what we now know to be its two-spinon contribution S_2 . First there has been the Anderson (semi-classical) spin-wave theory [6], an approach based on an expansion in powers of $1/s$, where s is the spin of the system and hence, is exact only in the classical limit $s = \infty$. It can describe with some satisfaction compounds with higher spins [7], but fails in the quantum limit $s = \frac{1}{2}$. Then there has been the so-called Müller ansatz [8], which gives an approximate expression for S_2 that can account for some aspects of the phenomenology for $s = \frac{1}{2}$ compounds. Only very recently could we get for this system a final exact expression for S_2 [9], and that gave a better account of the data [10].

Now for the spin- $\frac{1}{2}$ antiferromagnetic Heisenberg model, there is a need to go beyond the two-spinon contribution. The need is two-fold. First, it is important to see if one is able to get useful information from these complicated and compact expressions we alluded to above. Second and more important perhaps is the fact that, though the exact two-spinon contribution accounts for much of the phenomenology as we said¹, it still does not account for *all* of it. This point is demonstrated in particular in [11].

¹ About 70%, in a sense that will become clear later in section 3.

The natural step forward is to look into the exact four-spinon contribution. To the best of our knowledge, refs [12] and [13] constitute the first direct attempt in this direction. A general expression for the n -spinon contribution to the DCF in the anisotropic Heisenberg model is given in [13] and (a still compact one) for the isotropic limit in [12]. In ref [13], we specialize to the four-spinon case and give a discussion of some of its properties in the isotropic and Ising limits. In particular, we show that in the isotropic limit, the one of interest in this work, the exact four-spinon contribution is safe of any potential divergences.

In this work, we further the description of the four-spinon contribution S_4 . We show thus that it is actually possible to obtain sensible information from those complicated expressions. We determine the region in which S_4 is not identically zero and show that it is larger than that of S_2 . Also, we show that the behavior of S_4 as a function of the neutron momentum transfer k is similar in its overall shape to that of the corresponding S_2 , with differences though that we comment on.

The paper is organized as follows. In the next section, we briefly discuss the antiferromagnetic spin 1/2 Heisenberg model. We describe the spinon Hilbert-space structure and define the dynamical correlation function. In section 3, we succinctly review the properties of the two-spinon contribution. We give the exact expression of S_2 and that of the Müller ansatz, and briefly compare their main features. In section 4, we give the exact expression of S_4 and discuss in detail its properties we mentioned above. The last section comprises concluding remarks.

II. THE EXACT DCF IN THE XXX-MODEL

The antiferromagnetic $s = \frac{1}{2}$ XXX-Heisenberg model is defined as the isotropic limit of the XXZ -anisotropic Heisenberg Hamiltonian:

$$H_{XXZ} = -\frac{1}{2} \sum_{n=-\infty}^{\infty} (\sigma_n^x \sigma_{n+1}^x + \sigma_n^y \sigma_{n+1}^y + \Delta \sigma_n^z \sigma_{n+1}^z), \quad (1)$$

where $\Delta = (q + q^{-1})/2$ is the anisotropy parameter. The isotropic antiferromagnetic limit is obtained via the limit $q \rightarrow -1^+$ or equivalently $\Delta \rightarrow -1^-$. Here $\sigma_n^{x,y,z}$ are the usual Pauli matrices acting at the site n . The exact diagonalization directly in the thermodynamic limit of the Hamiltonian in (1) is possible using the $U_q(\widehat{sl(2)})$ quantum group symmetry present in the model [5]. The resulting Hilbert space \mathcal{F} consists of n -spinon energy eigenstates $|\xi_1, \dots, \xi_n\rangle_{\epsilon_1, \dots, \epsilon_n; i}$ built on the two vacuum states $|0\rangle_i$, $i = 0, 1$ such that²:

² The index i refers to the boundary condition on the spin chain, see [5].

$$H_{XXZ} |\xi_1, \dots, \xi_n\rangle_{\epsilon_1, \dots, \epsilon_n; i} = \sum_{j=1}^n e(\xi_j) |\xi_1, \dots, \xi_n\rangle_{\epsilon_1, \dots, \epsilon_n; i}, \quad (2)$$

where $e(\xi_j)$ is the energy of spinon j and ξ_j is a spectral parameter living on the unit circle. In the above equation, $\epsilon_j = \pm 1$. The translation operator T which shifts the spin chain by one site acts on the spinon eigenstates in the following manner:

$$T |\xi_1, \dots, \xi_n\rangle_{\epsilon_1, \dots, \epsilon_n; i} = \prod_{i=1}^n \tau(\xi_i) |\xi_1, \dots, \xi_n\rangle_{\epsilon_1, \dots, \epsilon_n; 1-i}, \quad (3)$$

where $\tau(\xi_j) = e^{-ip_j}$ and p_j is the lattice momentum of spinon j . The expressions of the spinon energy and lattice momentum in terms of the spectral parameter are quite cumbersome in the anisotropic case, see [5,13], but simplify considerably in the isotropic limit, see eq (11) below. The completeness relation in \mathcal{F} reads:

$$\mathbf{I} = \sum_{\mathbf{i}=\mathbf{0,1}} \sum_{\mathbf{n} \geq 0} \sum_{\{\epsilon_j = \pm 1\}_{j=1,n}} \frac{1}{\mathbf{n}!} \oint \prod_{j=1}^n \frac{d\xi_j}{2\pi i \xi_j} |\xi_1, \dots, \xi_n\rangle_{\epsilon_1, \dots, \epsilon_n; \mathbf{i}} \langle \xi_1, \dots, \xi_n| . \quad (4)$$

The two-point DCF is the Fourier transform of the zero-temperature vacuum-to-vacuum two-point function, i.e., it is defined by:

$$S^{i,+}(\omega, k) = \int_{-\infty}^{\infty} dt \sum_{m \in \mathbb{Z}} e^{i(\omega t + km)} {}_i \langle 0 | \sigma_m^+(t) \sigma_0^-(0) | 0 \rangle_i \quad (5)$$

where ω and k are the neutron energy and momentum transfer respectively and σ^\pm denotes $(\sigma^x \pm i\sigma^y)/2$. Inserting the completeness relation and using the Heisenberg relation:

$$\sigma_m^{x,y,z}(t) = \exp(iH_{XXZ}t) T^{-m} \sigma_0^{x,y,z}(0) T^m \exp(-iH_{XXZ}t), \quad (6)$$

we can write the transverse DCF as the sum of n -spinon contributions:

$$S^{i,+}(\omega, k) = \sum_{n \text{ even}} S_n^{i,+}(\omega, k), \quad (7)$$

where the n -spinon DCF S_n is given by:

$$S_n^{i,+}(\omega, k) = \frac{2\pi}{n!} \sum_{m \in \mathbb{Z}} \sum_{\epsilon_1, \dots, \epsilon_n} \oint \prod_{j=1}^n \frac{d\xi_j}{2\pi i \xi_j} e^{im(k + \sum_{j=1}^n p_j)} \delta \left(\omega - \sum_{j=1}^n e_j \right) \times X_{\epsilon_n, \dots, \epsilon_1}^{i+n}(\xi_n, \dots, \xi_1) X_{\epsilon_1, \dots, \epsilon_n}^{1-i}(-q\xi_1, \dots, -q\xi_n), \quad (8)$$

relation in which X^i denotes the form factor:

$$X_{\epsilon_1, \dots, \epsilon_n}^i(\xi_1, \dots, \xi_n) \equiv {}_i \langle 0 | \sigma_0^+(0) | \xi_1, \dots, \xi_n \rangle_{\epsilon_1, \dots, \epsilon_n; i} . \quad (9)$$

The exact expression of this form factor has been determined in [5]. Using this form factor, we can give an exact expression for the n -spinon DCF in the anisotropic case, see [13], and determine exactly its isotropic limit, see [12]. This limit is obtained via the replacement [5,13]:

$$\xi = ie^{-2i\varepsilon\rho}; \quad q = -e^{-\varepsilon}, \quad \varepsilon \rightarrow 0^+, \quad (10)$$

where ρ is the spectral parameter suited for this limit. The expressions of the energy e and momentum p in terms of ρ then read:

$$e(\rho) = \frac{\pi}{\cosh(2\pi\rho)} = -\pi \sin p; \quad \cot p = \sinh(2\pi\rho); \quad -\pi \leq p \leq 0. \quad (11)$$

The transverse two-spinon DCF S_2 does not involve a contour integration and has been given in [9]. The four-spinon one S_4 involves only one contour integration and its expression is given in [13]. In the next section, we review the properties of S_2 and in the one that follows it, we discuss those of S_4 .

III. THE EXACT TWO-SPINON DCF

The exact expression of the two-spinon DCF of the spin $\frac{1}{2}$ XXX -model is given in [9] and reads:

$$S_2^{+-}(\omega, k - \pi) = \frac{1}{4} \frac{e^{-I(\rho)}}{\sqrt{\omega_{2u}^2 - \omega^2}} \Theta(\omega - \omega_{2l}) \Theta(\omega_{2u} - \omega), \quad (12)$$

where Θ is the Heaviside step function and the function $I(\rho)$ is given by:

$$I(\rho) = \int_0^{+\infty} \frac{dt}{t} \frac{\cosh(2t) \cos(4\rho t)}{\sinh(2t) \cosh(t)} e^t. \quad (13)$$

$\omega_{2u(l)}$ is the upper (lower) bound of the two-spinon excitation energies called the des Cloizeaux and Pearson [8,9] upper (lower) bound or limit. They read:

$$\omega_{2u} = 2\pi \sin \frac{k}{2}; \quad \omega_{2l} = \pi |\sin k|. \quad (14)$$

The quantity $\rho = \rho_1 - \rho_2$ and is related to ω and k by the relation:

$$\cosh \pi\rho = \sqrt{\frac{\omega_{2u}^2 - \omega_{2l}^2}{\omega^2 - \omega_{2l}^2}}, \quad (15)$$

a relation obtained using eq (11) and the energy-momentum conservation laws:

$$\omega = e_1 + e_2; \quad k = -p_1 - p_2. \quad (16)$$

The properties of S_2 have been discussed in [10]. There, a comparison with the Müller ansatz [8] is given. This latter was derived from the properties of some solutions to the Bethe-ansatz equations, from numerical calculations on finite spin chains and from an analysis of phenomenological results. It reads:

$$S_2^{(a)}(\omega, k - \pi) = \frac{A}{2\pi} \frac{\Theta(\omega - \omega_{2l}) \Theta(\omega_{2u} - \omega)}{\sqrt{\omega^2 - \omega_{2l}^2}} , \quad (17)$$

where A is a constant determined in such a way to fit best the phenomenology [8]. There are two main differences between the exact expression (12) and the approximate one (17), [10]. First, the two-spinon threshold at ω_{2l} is more singular in (12) than in (17). Second, at the upper two-spinon boundary ω_{2u} , S_2 vanishes smoothly whereas $S_2^{(a)}$ has a sharp cut-off. But if one defines the frequency moments of the DCF:

$$K_n(k) = \int_{-\infty}^{+\infty} d\omega \omega^n S(\omega, k) , \quad (18)$$

one shows that as $k \rightarrow 0$, the moment of S_2 vanishes as:

$$K_n^{(2)}(k) \sim \omega_{2u}^{n+1}(k) , \quad (19)$$

and the same holds for the Müller ansatz $S_2^{(a)}$.

Actually, the frequency moments (18) are particular cases of a set of general sum rules the DCF is known to satisfy some of them exactly. For example, we know that the first moment is exactly equal to [14]:

$$K_1(k) = \frac{4 \ln 2 - 1}{6} (1 - \cos k) . \quad (20)$$

It turns out that the same frequency moment for S_2 is such that [10] :

$$\frac{K_1^{(2)}(k)}{K_1(k)} \simeq 70\% . \quad (21)$$

This means that, according to this sum rule, S_2 is way off the total DCF S by roughly 30%. In fact, other exact sum rules confirm this trend, see [10]. Of course, those remaining 30% are “filled”, so to speak, by the $n > 2$ -spinon contributions. The natural question that comes to mind is: how much S_4 takes up from these 30%? We comment on this issue in the last section.

IV. THE EXACT FOUR-SPINON DCF

The analytic expression of the four-spinon DCF has been worked out in [13]. It reads:

$$S_4^{+-}(\omega, k - \pi) = C_4 \int_{-\pi}^0 dp_3 \int_{-\pi}^0 dp_4 F(\rho_1, \dots, \rho_4) , \quad (22)$$

where C_4 is a numerical constant and the integrand F is given by:

$$F(\rho_1, \dots, \rho_4) = \sum_{(p_1, p_2)} \frac{f(\rho_1, \dots, \rho_4) \sum_{\ell=1}^4 |g_\ell(\rho_1, \dots, \rho_4)|^2}{\sqrt{W_u^2 - W^2}} . \quad (23)$$

The different quantities involved in this expression are:

$$\begin{aligned} W &= \omega + \pi (\sin p_3 + \sin p_4) ; \\ W_u &= 2\pi \left| \sin \frac{K}{2} \right| ; \\ K &= k + p_3 + p_4 ; \\ \cot p_j &= \sinh(2\pi\rho_j) , \quad -\pi \leq p_j \leq 0 . \end{aligned} \quad (24)$$

The function f is given by:

$$f(\rho_1, \dots, \rho_4) = \exp \left[- \sum_{1 \leq j < j' \leq 4} I(\rho_j - \rho_{j'}) \right] , \quad (25)$$

and the function g_ℓ reads:

$$\begin{aligned} g_\ell &= (-1)^{\ell+1} (2\pi)^4 \sum_{j=1}^4 \cosh(2\pi\rho_j) \\ &\times \sum_{m=\Theta(j-\ell)}^{\infty} \frac{\prod_{i \neq \ell} (m - \frac{1}{2}\Theta(\ell - i) + i\rho_{ji})}{\prod_{i \neq j} \pi^{-1} \sinh(\pi\rho_{ji})} \prod_{i=1}^4 \frac{\Gamma(m - \frac{1}{2} + i\rho_{ji})}{\Gamma(m + 1 + i\rho_{ji})} , \end{aligned} \quad (26)$$

where Θ is the Heaviside step function and $\rho_{ji} = \rho_j - \rho_i$. In (23), the sum $\sum_{(p_1, p_2)}$ is over the two pairs (p_1, p_2) and (p_2, p_1) solutions of the energy-momentum conservation laws:

$$W = -\pi(\sin p_1 + \sin p_2) ; \quad K = -p_1 - p_2 . \quad (27)$$

They read:

$$(p_1, p_2) = \left(-\frac{K}{2} + \arccos \left(\frac{W}{2\pi \sin \frac{K}{2}} \right) , \quad -\frac{K}{2} - \arccos \left(\frac{W}{2\pi \sin \frac{K}{2}} \right) \right) . \quad (28)$$

Note that the solution in (28) is allowed as long as $W_l \leq W \leq W_u$ where W_u is given in (24) and:

$$W_l = \pi |\sin K| . \quad (29)$$

In the work [13], we have discussed the behavior of the function F given in (23). We have shown that the series g_ℓ is convergent. We have also shown that in the region where two ρ_i 's or more get equal, the function g_ℓ is finite. The function f going to zero in these same regions [10], this means the integrand F of S_4 has a nice regular behavior there. Furthermore, we have shown that F is exponentially convergent when one of the ρ_i 's goes to infinity, which means the two integrals over p_3 and p_4 in (22) do not yield infinities. All these analytic results pave the way to “safe” numerical manipulations.

The first thing we wish to discuss in this work is the extent of the region in the (k, ω) -plane in which S_4 is not identically zero, and compare it to that of S_2 . Remember that from (12), S_2 is zero identically outside the spin-wave continuum $\omega_{2l}(k) \leq \omega \leq \omega_{2u}(k)$, where $\omega_{2l,u}(k)$ are given in (14). From the condition $W_l \leq W \leq W_u$ discussed after eq (28), one infers that for example in the interval $0 \leq k \leq \pi$, in order for S_4 to be nonzero identically, one has to have $\omega_{4l} \leq \omega \leq \omega_{4u}$, where:

$$\begin{aligned}\omega_{4l}(k) &= 3\pi \sin(k/3) \quad \text{for } 0 \leq k \leq \pi/2; \\ \omega_{4l}(k) &= 3\pi \sin(k/3 + 2\pi/3) \quad \text{for } \pi/2 \leq k \leq \pi; \\ \omega_{4u}(k) &= 4\pi \cos(k/4) \quad \text{for } 0 \leq k \leq \pi.\end{aligned}\tag{30}$$

All these branches extend to the interval $\pi \leq k \leq 2\pi$ by symmetry with respect to the axis $k = \pi$ and are plotted in fig. 1.

The first thing we immediately see is that the S_4 -region, i.e., the region in which S_4 is not identically zero, is not confined to the spin-wave continuum delimited by the dCP branches $\omega_{2l,u}$ given in (14). This means that, a fortiori, the full S is also not confined to the S_2 -region. This fact is confirmed by early finite chain numerical calculations [8] and the phenomenology [2].

Furthermore, fig. 1 shows that for $0 \leq k/\pi \leq 1/2$ and $3/2 \leq k/\pi \leq 2$, the S_4 -region is entirely beyond the S_2 -region. This means that for these intervals, we may expect S_2 to be dominant in S within the spin-wave continuum. However, for $1/2 \leq k/\pi \leq 3/2$, there is overlap between the two regions such that the S_2 -region is more or less within the S_4 -region. We may therefore expect here the contribution of S_4 to play a rôle, and hence, we expect S_2 to be a little less dominant within the spin-wave continuum.

The next feature we discuss in this work is the behavior of S_4 as a function of k for fixed ω . Figs. 2a, 3a, 4a and 5a show the behavior of S_4 for $\omega/\pi = 0.45, 0.5, 0.75$ and 1 respectively. Note that we have scaled S_4 to appropriate units. Figs. 2b, 3b, 4b, and 5b show the behavior of S_2 as a function of k for the same values of ω . As one can see from the figures, the discussion of the case $\omega/\pi = 0.45$ parallels that of the case $\omega/\pi = 0.5$, and that of the case $\omega/\pi = 0.75$ that of $\omega/\pi = 1$.

Let us first discuss the case $\omega/\pi = 1/2$. We see from fig. 3b that the function S_2 vanishes

outside (roughly) the interval $0.8 \leq k/\pi \leq 1.2$. Looking back into fig. 1, this corresponds indeed to the region inside the spin-wave continuum that corresponds to $\omega/\pi = 1/2$, i.e., $5/6 \leq k/\pi \leq 7/6$. The function S_2 starts at $k/\pi = 5/6$ with a large (infinite) value and goes to a minimum at $k/\pi = 1$; it then increases back to infinity at $k/\pi = 7/6$. Fig. 3a shows that the function S_4 has a somewhat similar behavior, with one important difference though, a difference we discuss in a moment. From the figure, we read that S_4 vanishes outside (roughly) the interval $0.8 \leq k/\pi \leq 1.2$. From fig. 1, that corresponds within the S_4 -region to the interval $0.84 \leq k/\pi \leq 1.16$. But fig. 1 shows also that for $\omega/\pi = 1/2$, S_4 may be non-vanishing in the two intervals $0 \leq k/\pi \leq 0.16$ and $1.84 \leq k/\pi \leq 2$. That contribution doesn't appear on fig. 3a, presumably because S_4 there is negligible. This is confirmed in the case $\omega/\pi = 0.45$, where we see S_4 having a very small contribution in the corresponding intervals.

Also, from fig. 3a we see that S_4 like S_2 starts from a large (infinite) value at its lower boundary $k/\pi = 0.84$, goes to a minimum and increases back to a large (infinite) value at the upper boundary $k/\pi = 1.16$. But as we said, there is one important difference³. Indeed, the symmetry about the $k = \pi$ axis, present in the case of S_2 , appears to be lost for S_4 , and hence for the total S . The same feature happens in the case $\omega/\pi = 0.45$.

We turn to the case $\omega/\pi = 1$. Fig. 5b shows S_2 starting from zero at roughly $k/\pi = 0.3$, getting to a maximum and sharply dropping to zero at roughly $k/\pi = 0.5$. It then starts sharply from a large (infinite) value and decreases to a minimum at $k/\pi = 1$. Its behavior in the other interval $1 \leq k/\pi \leq 2$ is the symmetric of that in the interval $0 \leq k/\pi \leq 1$ we just described. This is also consistent with fig. 1: the function S_2 starts to be non-vanishing for $\omega/\pi = 1$ at $k/\pi = 1/3$. It stays nonvanishing until k reaches $\pi/2$ where ω touches on the lower boundary, and hence S_2 vanishes. Passed that point, it restarts to be nonvanishing with the behavior we described.

What is interesting is that S_4 has in this case too the same overall behavior as that of S_2 , but here again with differences we comment on a little later. In fig. 5a, we see that S_4 starts to increase from the value zero at $k = 0$. It goes quickly to a maximum before dropping sharply to zero a little before $k/\pi = 0.5$. It stays at zero till a little after $k/\pi = 0.5$ and increases sharply to infinity. Then it decreases while wiggling, regaining a local maximum at about $k/\pi = 1$. Its behavior on the other side of the axis $k = \pi$ is similar to the one on the side we just described. This overall behavior is also consistent with fig. 1. Indeed, for $\omega/\pi = 1$, the S_4 -region starts at $k = 0$ and extends first to $k/\pi = 0.3245$. Then we get

³We remind the reader that, for the sake of the discussion, S_4 is plotted scaled to appropriate units.

outside this region from this value of k till $k/\pi = 0.6755$. Then S_4 is no more identically zero beyond this point until we reach the symmetric of the point $k/\pi = 0.6755$ with respect to the axis $k = \pi$. It becomes identically zero from this point until the one symmetric to $k/\pi = 0.3245$. From this point to $k/\pi = 2$, it is not identically zero. As we said, this is quite consistent with fig. 5a.

The differences between S_4 and S_2 in the case $\omega/\pi = 1$ are the following. The symmetry about the $k/\pi = 1$ axis, present in the case of S_2 , is here also somewhat lost, but not in the overall shape, rather in the detail, as in the cases $\omega/\pi = 0.45$ and $\omega/\pi = 1/2$. Second, in S_2 , the point $k/\pi = 1$ is a minimum while in S_4 , it seems to be a local maximum. This is not the case for $\omega/\pi = 0.45$ and $\omega/\pi = 1/2$. Finally, the shape of S_4 is more “wiggly” than that of S_2 .

As to the wiggles in the shape of S_4 , we would like to add a comment. The numerics as far as S_4 is concerned are a lot more involved than those for S_2 . Thus, we are tempted to say that part of that “wiggling” may be due to this fact. Of course, this doesn’t rule out by any means a real physical origin. It just maybe that the real effect is less dramatic than how it looks on figs. 5a and 4a.

V. DISCUSSION AND CONCLUSION

In this work, we have discussed the behavior of the exact four-spinon contribution S_4 to the dynamical correlation function S of the $s = 1/2$ antiferromagnetic Heisenberg model and compared it to the one of the exact two-spinon contribution S_2 . We first reviewed the model and the spinon structure of the corresponding Hilbert space. We then gave a brief account of the results concerning S_2 and its comparaison to the Müller ansatz. The first thing concerning S_4 we discussed is the region in the (k, ω) -plane in which S_4 is not identically zero. We found it to be different and larger than that of S_2 , i.e., the spin-wave continuum. Both regions are drawn in fig. 1. We then discussed the behavior of S_4 as a function of k for fixed values of ω , and compared it to the one of S_2 . These behaviors are plotted in figs. 2,3,4 and 5. We have found that the overall shape of S_4 is more or less the same as that of S_2 . However, the symmetry about the $k = \pi$ axis, present in the case of S_2 , seems to be lost in the case of S_4 , which means that it should also be lost in the case of the total S . Also, the S_4 -curves are generally more wiggled than those of S_2 . We have pointed out that we think this wiggling is partly due to the more complicated S_4 -numerics.

It would have been interesting to measure S_4 for other (larger) values of ω , especially in regions where S_2 is identically zero whereas S_4 is not, see fig. 1. But as ω increases, the structure of the function $F(\rho_1, \dots, \rho_4)$ of eq(23) in the (p_3, p_4) -plane gets “richer”, which means numerically harder to handle. To illustrate this point, we have plotted for the reader

in figs. 6 the function F for $k/\pi = 1/2$ and four different values of ω . One can see that as ω increases, the functions F gets distributed nontrivially⁴ in larger areas in the (p_3, p_4) -plane, with an increasing more involved structure. This is the main reason why we prefered to defer the discussion of these regions to future work. Also, for the same reason, we have defered the systematic discussion of S_4 as a function of ω for fixed values k .

One other interesting question we haven't touched on in this work but merely alluded to at the end of section 3 is the following: how much S_4 accounts for in the total S ? In other words, is $S_2 + S_4$ better an approximation to the total S than S_2 alone, and if yes, by how much? As we said, we know that S_2 accounts for about 70% of the total S , which means that roughly 30% are left for the $n > 2$ -spinon contributions. To tackle this question as it should, one has to rely on a certain number of sum rules S is known to satisfy exactly. Then one compares the contribution of $S_2 + S_4$ to the exact result and carries a discussion thereon.

The other interesting question one may ask is the physical interpretation and implications of the behavior of the four-spinon DCF we have described in this work. What would certainly be interesting is to be able to systematically measure S outside the spin-wave continuum so that we are assured of having the effects of the two-spinon contribution eliminated.

ACKNOWLEDGEMENTS

We would like to thank Asmaa Abada and Joaquim Matias for all their help.

⁴Never mind the units of F , we have scaled it appropriately.

REFERENCES

- [1] Some (not *all*) of the literature related to the Heisenberg model, our interest in this work, comprises W. Heisenberg, *Z. Phys.* 49 (1928) 619; H. Bethe, *Z. Phys.* 71 (1931) 205; L. Hulthén, *Arkiv. Mat. Astron. Fysik A* 1126 (1938) 1; E.H. Lieb and D.C. Mattis, *J. Math. Phys.* 3 (1962) 749; J. des Cloizeaux and J.J. Pearson, *Phys. Rev.* 128 (1962) 2131; R.B. Griffiths, *Phys. Rev.* 133 (1964) A 768; C.N. Yang and C.P. Yang, *Phys. Rev.* 150 (1966) 321; 150 (1966) 327; 151 (1966) 258; Th. Niemeijer, *Physica* 36 (1967) 377; E. Barouch, B.M. McCoy and D.B. Abraham, *Phys. Rev.* **A4** (1971) 2331; M. Gaudin, *Phys. Rev. Lett.* 26 (1971) 1301; M. Takahashi, *Prog. Theor. Phys.* 46 (1971) 401; L.A. Takhtajan and L.D. Faddeev, *Russ. Math. Surveys* 34 (1979) 11; B.M. McCoy, J.H.H. Perk and R.E. Shrock, *Nucl. Phys.* **B220** (1983) 35; O. Babelon, H.J. de Vega and C.M. Viallet, *Nucl. Phys.* **B220** (1983) 13; G. Müller and R.E. Shrock, *Phys. Rev.* **B29** (1984) 288; J.M.R. Roldan, B.M. McCoy and J.H.H. Perk, *Physica* 136A (1986) 255; V.E. Korepin, A.G. Izergin and N.M. Bogoliubov, ‘*The Quantum Inverse Scattering Method and Correlation Functions*’, Cambridge University Press, 1993; F.H.L. Essler, H. Frahm, A.G. Izergin and V.E. Korepin, *Comm. Math. Phys.* 174 (1994) 191; V.E. Korepin, A.G. Izergin, F.H.L. Essler and D. Uglov, *Phys. Lett.* **A190** (1994) 182.
- [2] D.A. Tennant, R.A. Cowley, S.E. Nagler and A.M. Tsvelik, *Phys. Rev.* **B52** (1995) 13368; D.A. Tennant, S.E. Nagler, D. Weltz, G. Shirane and K. Yamada, *Phys. Rev.* **B52** (1995) 13381; D.A. Tennant, T.G. Perring, R.A. Cowley and S.E. Nagler, *Phys. Rev. Lett.* 70 (1993) 4003; S.E. Nagler, D.A. Tennant, R.A. Cowley, T.G. Perring and S.K. Satija, *Phys. Rev.* **B44** (1991) 12361.
- [3] R.J. Baxter, ‘*Exactly Solved Models in Statistical Mechanics*’, Academic Press, 1982.
- [4] O. Davies, O. Foda, M. Jimbo, T. Miwa and A. Nakayashiki, *Comm. Math. Phys.* 151 (1993) 89; for the techniques of bosonization on quantum affine algebras, see for example I.B. Frenkel and N.H. Jing, *Proc. Natl. Acad. Sci.* 85 (1988) 9373; A. Abada, A.H. Bougourzi and M.A. El Gradechi, *Mod. Phys. Lett.* A8 (1993) 715; A.H. Bougourzi, *Nucl. Phys.* **B404** (1993) 457, and more recently A.H. Bougourzi, ‘*Bosonization of quantum affine groups and its application to the higher spin Heisenberg model*’, ITP-SB-97-29, q-alg/9706015.
- [5] M. Jimbo and T. Miwa, ‘*Algebraic Analysis of Solvable Lattice Models*’, American Mathematical Society, 1994.
- [6] P.W. Anderson, *Phys. Rev.* 86 (1952) 694.
- [7] M.T. Hutchings, G. Shirane, R.J. Birgeneau and S.L. Holt, *Phys. Rev.* **B5**, (1972) 1999.

- [8] G. Müller, H. Thomas, H. Beck and J.C. Bonner, Phys. Rev. **B24** (1981) 1429.
- [9] A.H. Bougourzi, M. Couture and M. Kacir, Phys. Rev. **B** 54 (1996) 12669.
- [10] M. Karbach, G. Müller and A.H. Bougourzi, ‘*Two-spinon dynamic structure factor of the one-dimensional $S = 1/2$ Heisenberg antiferromagnet*’, [cond-mat/9606068](https://arxiv.org/abs/cond-mat/9606068).
- [11] A. Fledderjohann, K.H. Mütter and M. Karbach and G. Müller, ‘*Significance of the non-2-spinon part of $S(q, \omega)$ in the one dimensional $S = 1/2$ Heisenberg antiferromagnet at zero-temperature*’, [cond-mat/9607102](https://arxiv.org/abs/cond-mat/9607102).
- [12] A.H. Bougourzi, Mod. Phys. Lett **B10** (1996) 1237.
- [13] A. Abada, A.H. Bougourzi and B. Si-lakhal, Nucl. Phys. **B497** [FS] (1997) 733.
- [14] P.C. Hohenberg and W.F. Brinkman, Phys. Rev. **B10** (1974) 128.

Figure captions

Fig. 1: The regions in the (k, ω) -plane inside which S_2 (dashed lines) and S_4 (solid lines) are not identically zero. The boundaries are indicated as defined in the text.

Figs. 2–5: S_4 (a) and S_2 (b) as functions of k for fixed ω . The values of ω are indicated. Note that S_4 is plotted to appropriate units.

Figs. 6: The function $F(\rho_1, \dots, \rho_4)$ of relation (22) plotted in the (p_3, p_4) -plane for $k = 0.5\pi$ and different values of ω as indicated. Note that F is scaled to appropriate units.

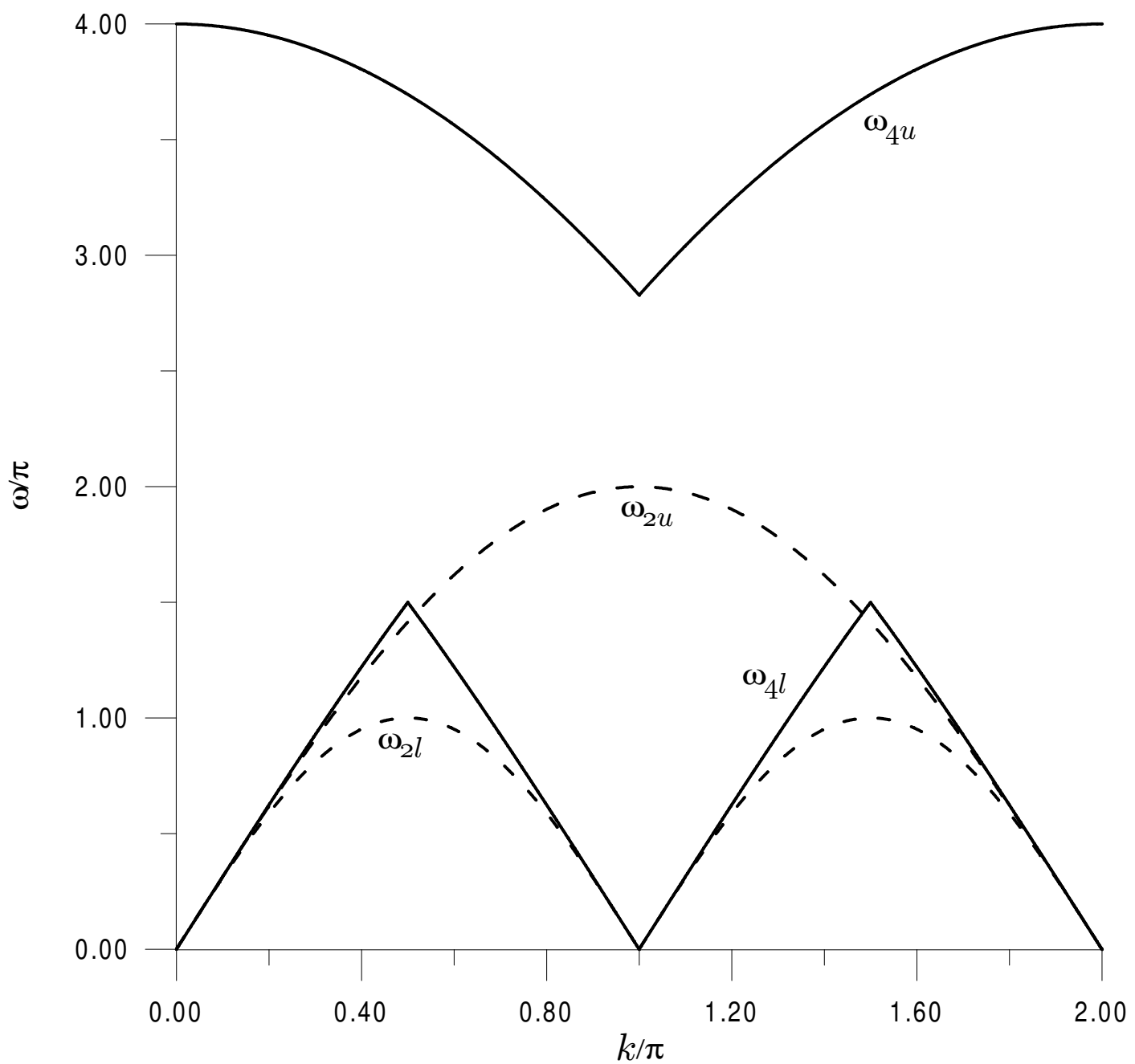


figure 1

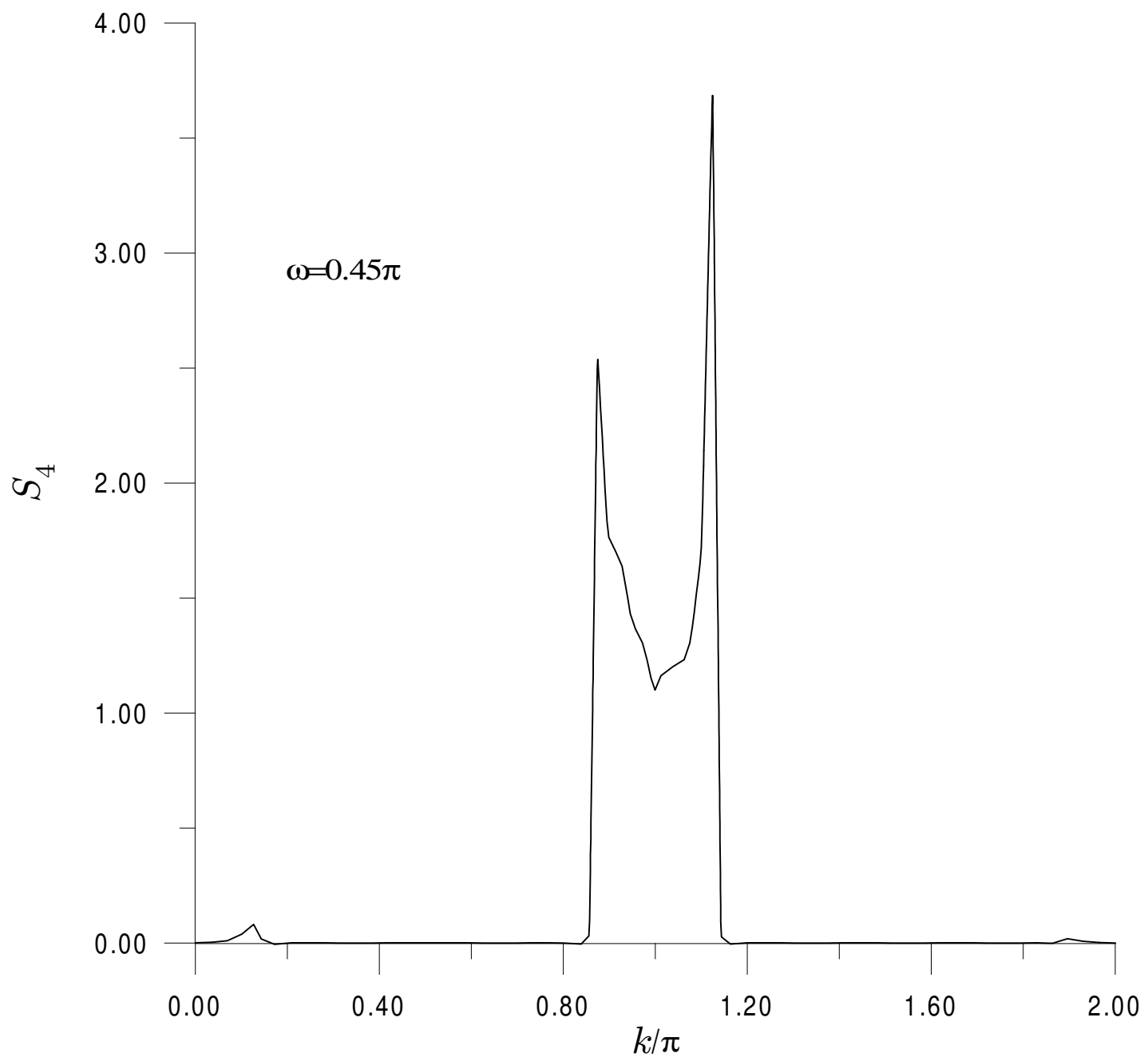


figure 2a

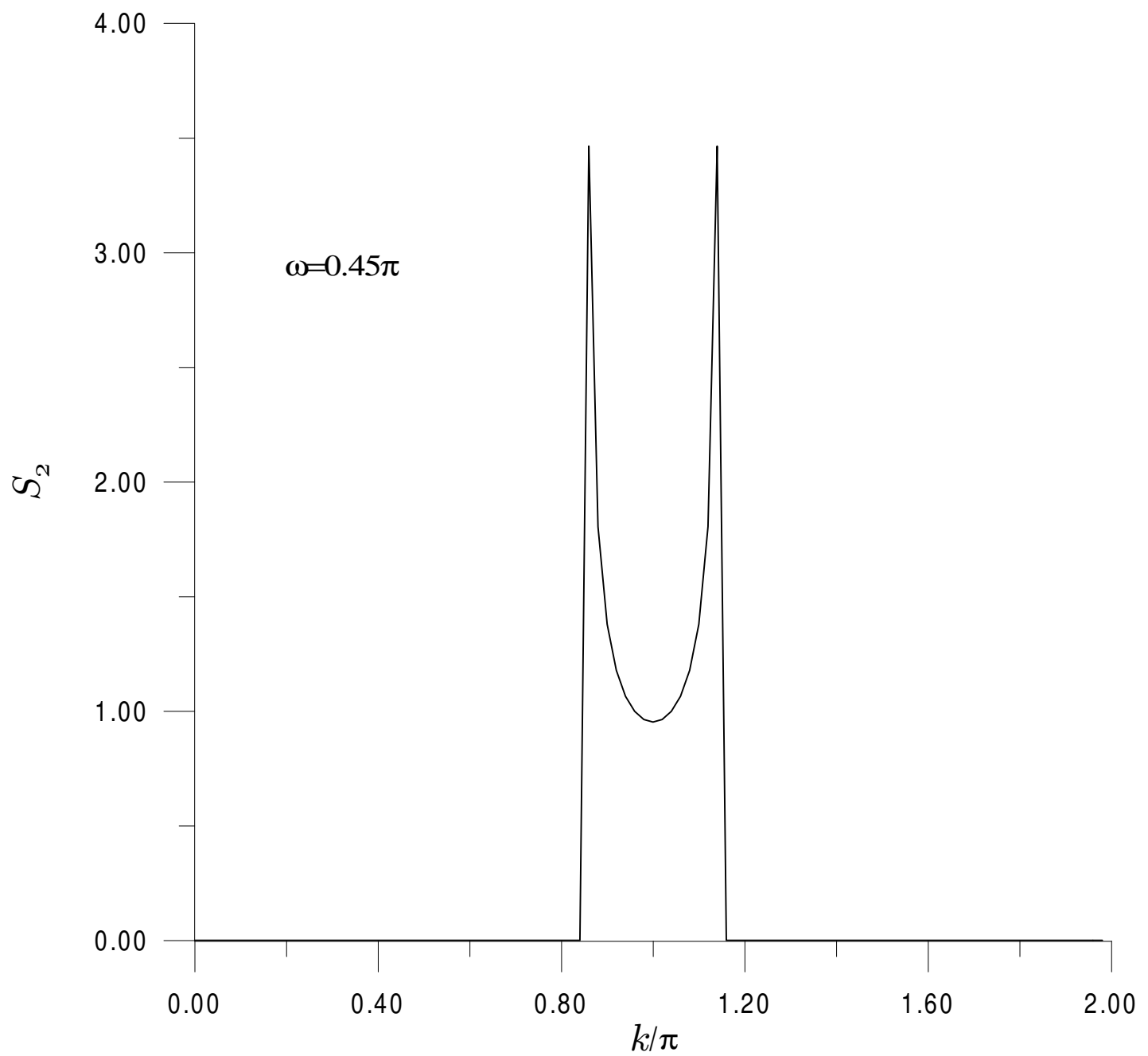


figure 2b

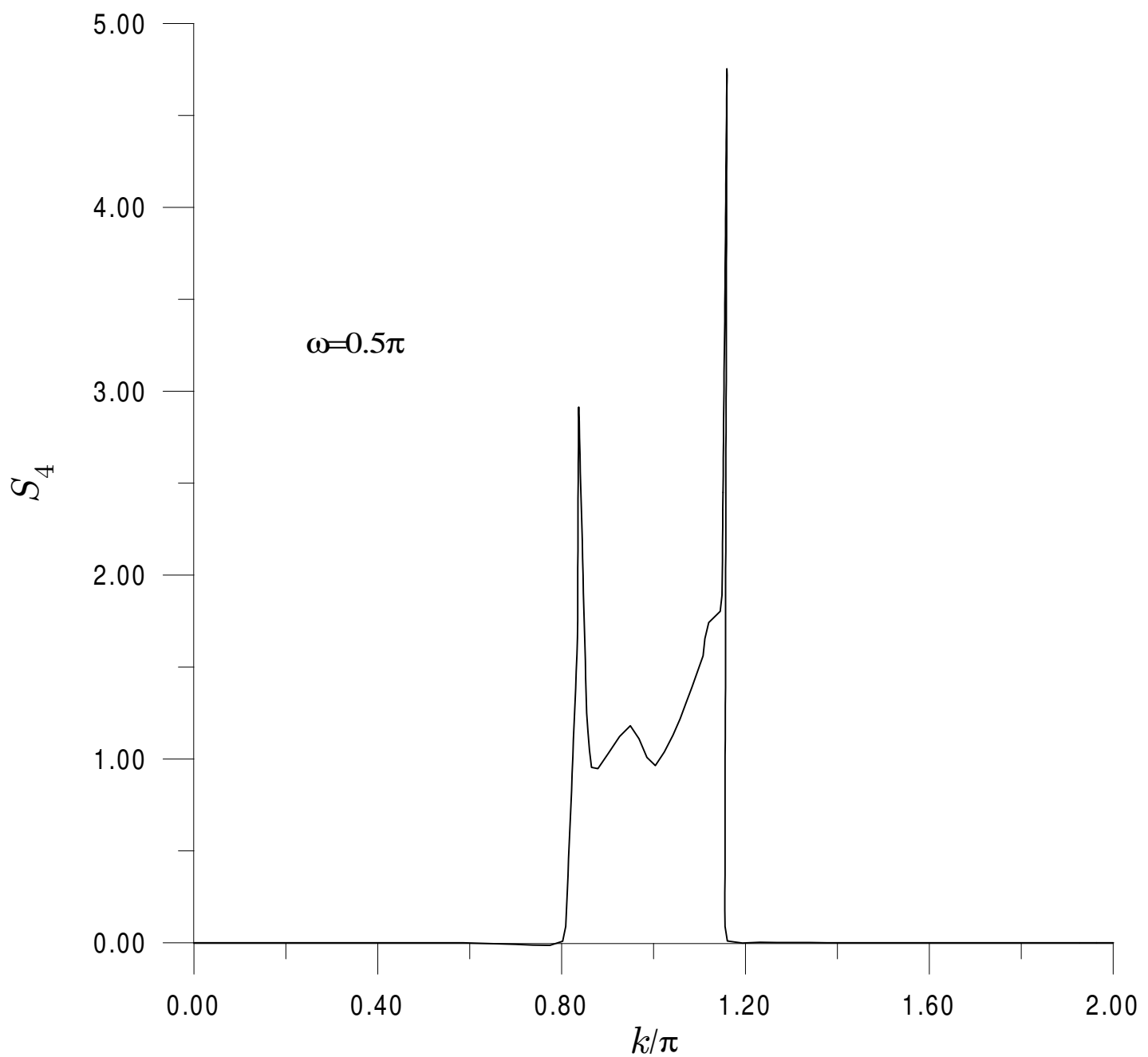


figure 3a

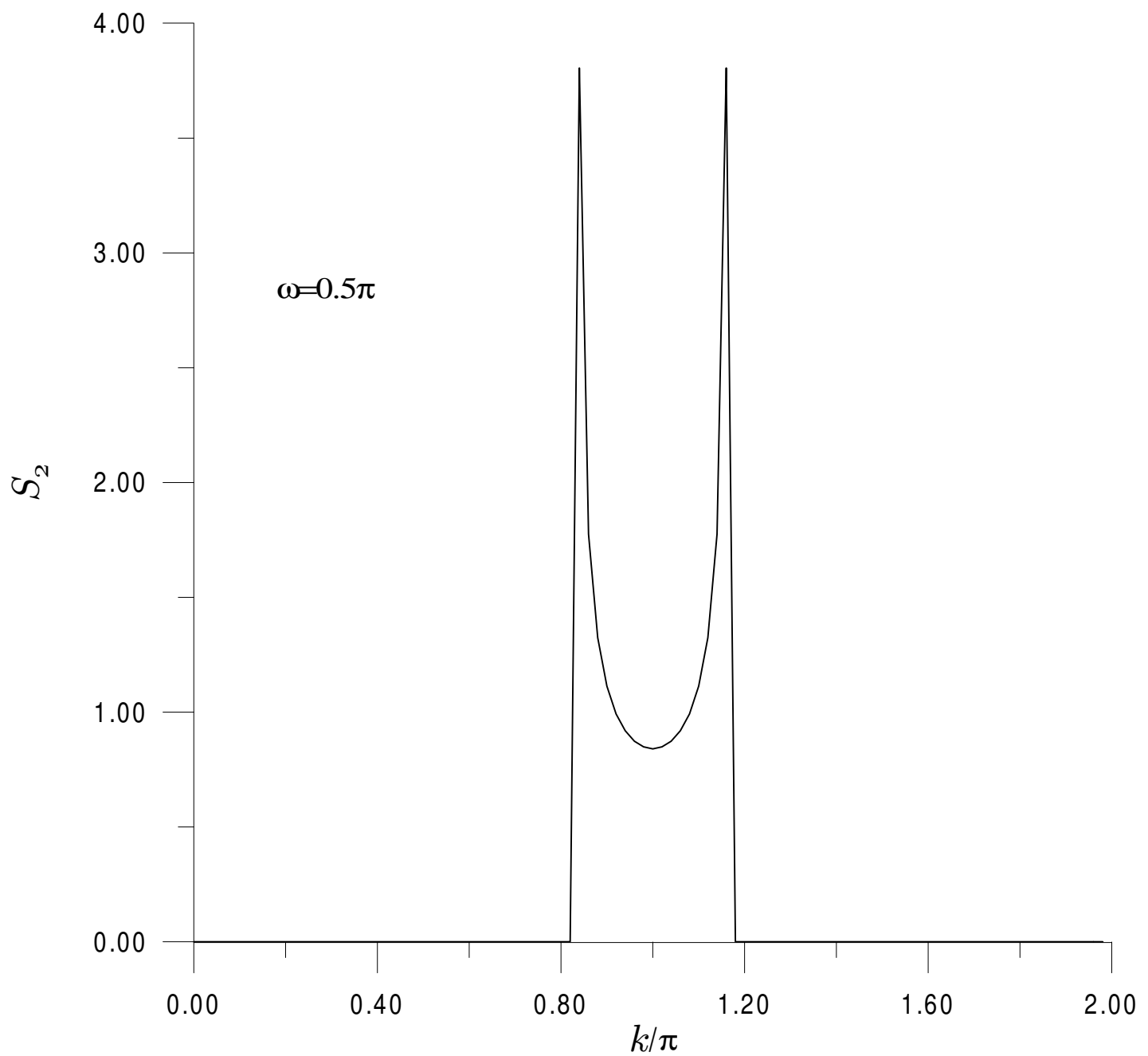


figure 3b

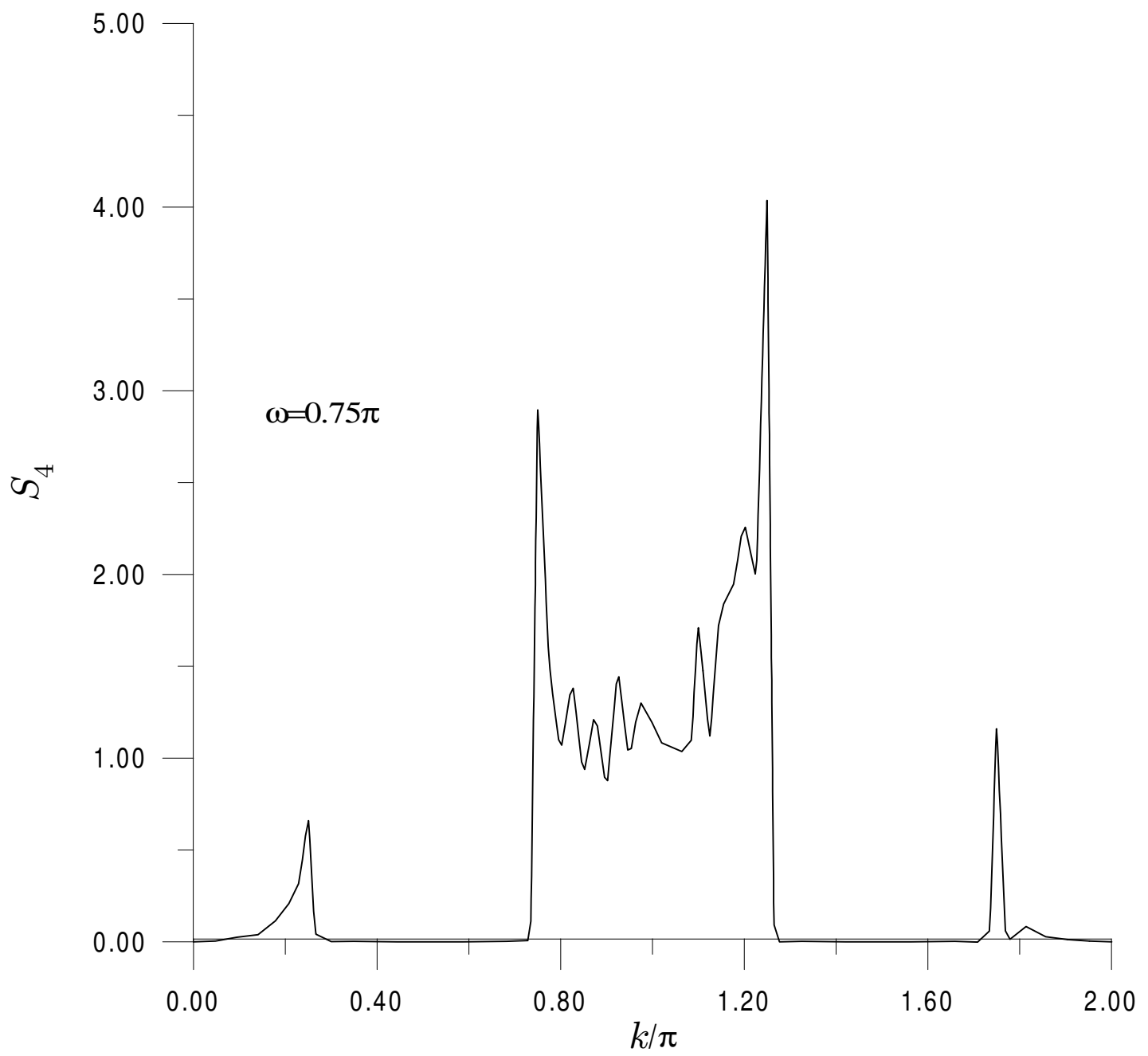


figure 4a

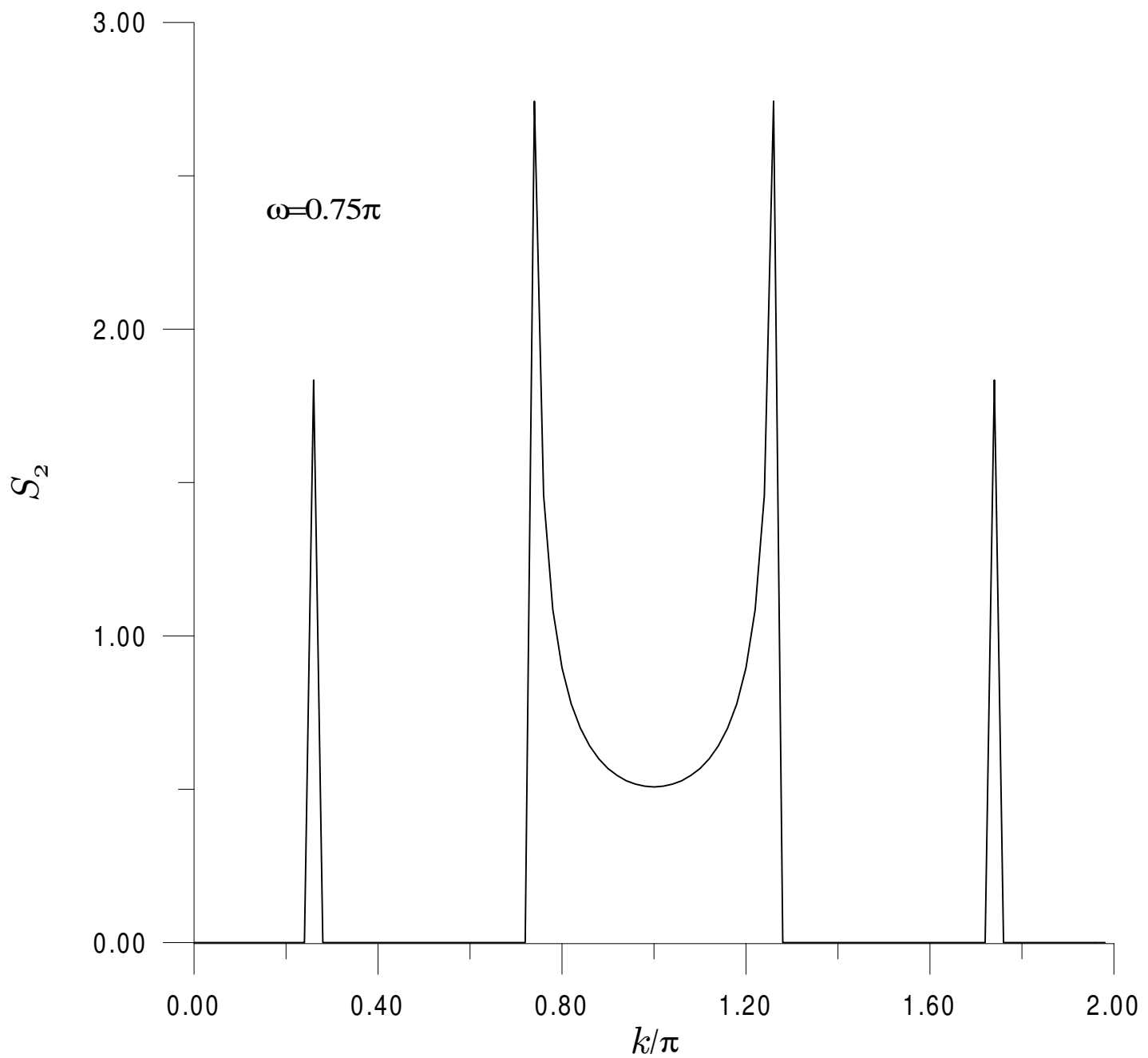


figure 4b

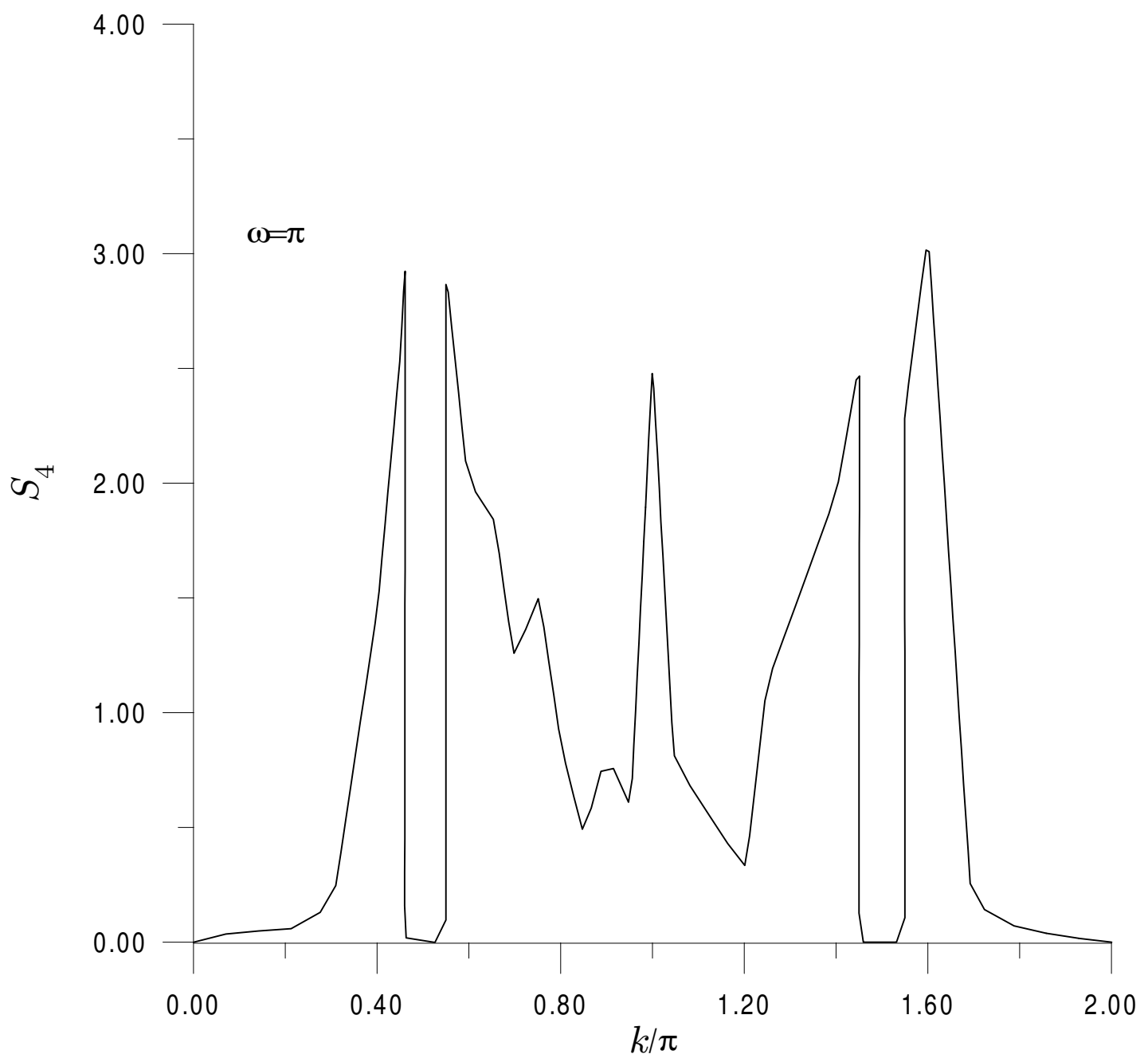


figure 5a

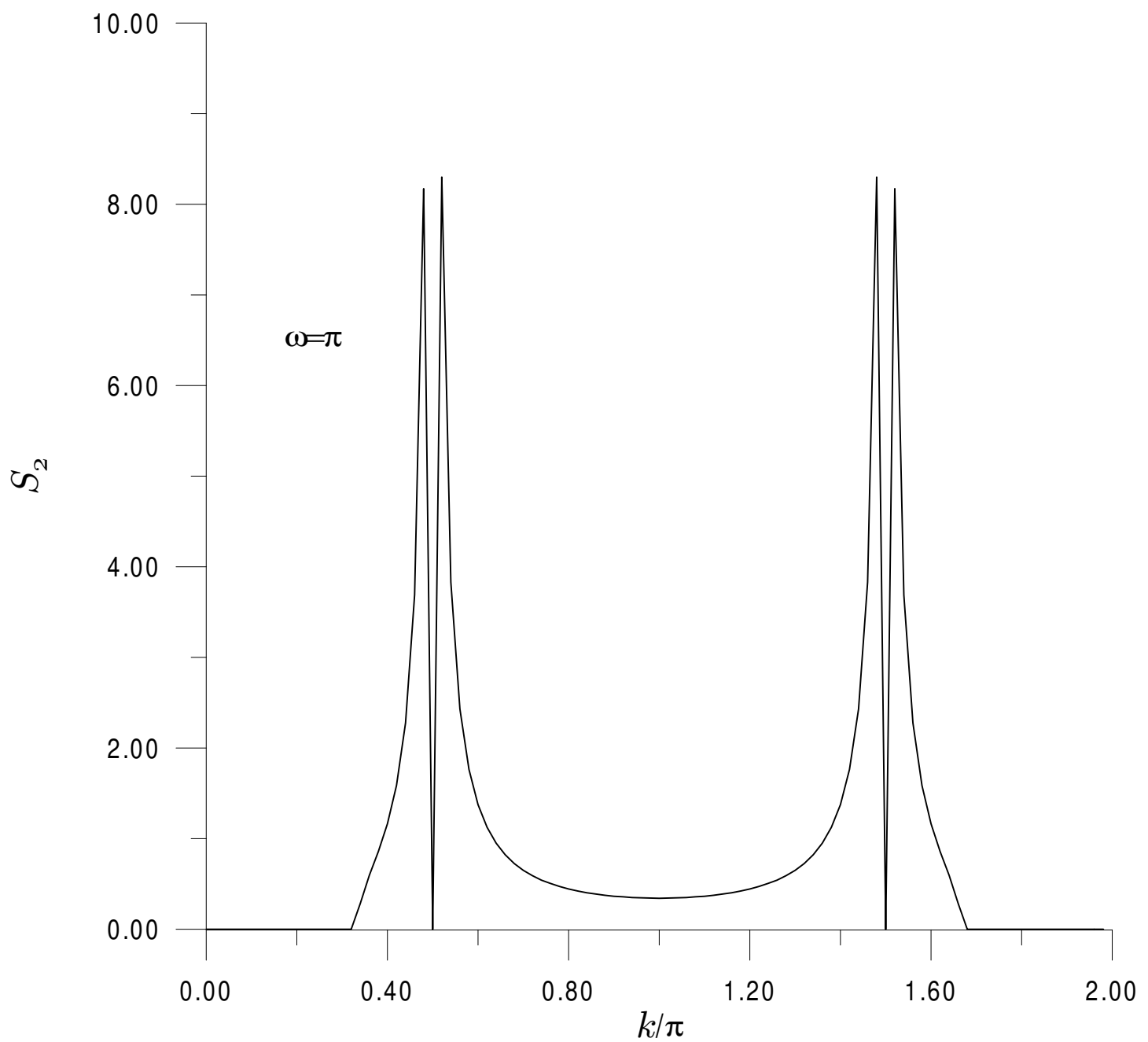


figure 5b

$$k=0.5\pi$$
$$\omega=1.2\pi$$

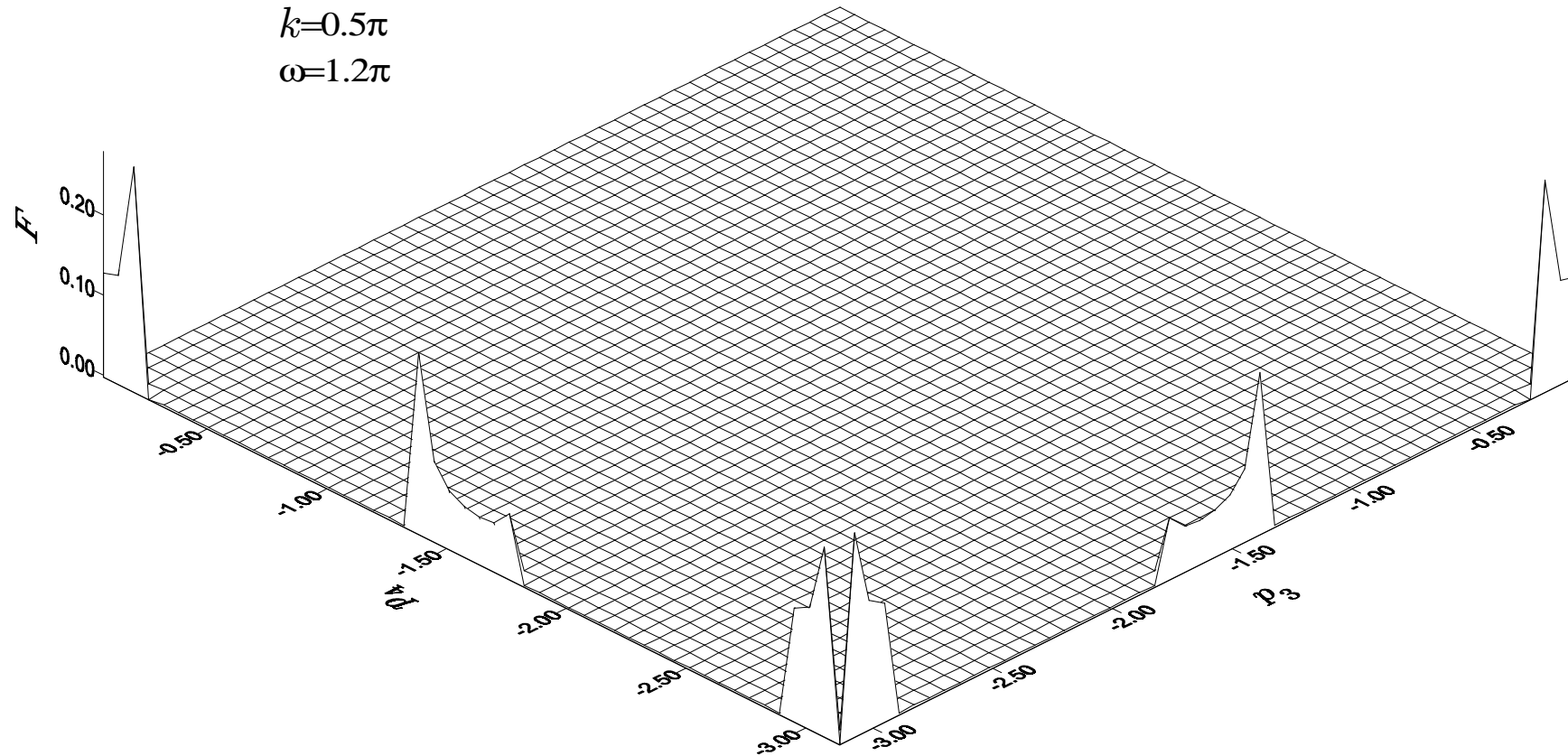


figure 6a

$$\begin{aligned}k &= 0.5\pi \\ \omega &= 2\pi\end{aligned}$$

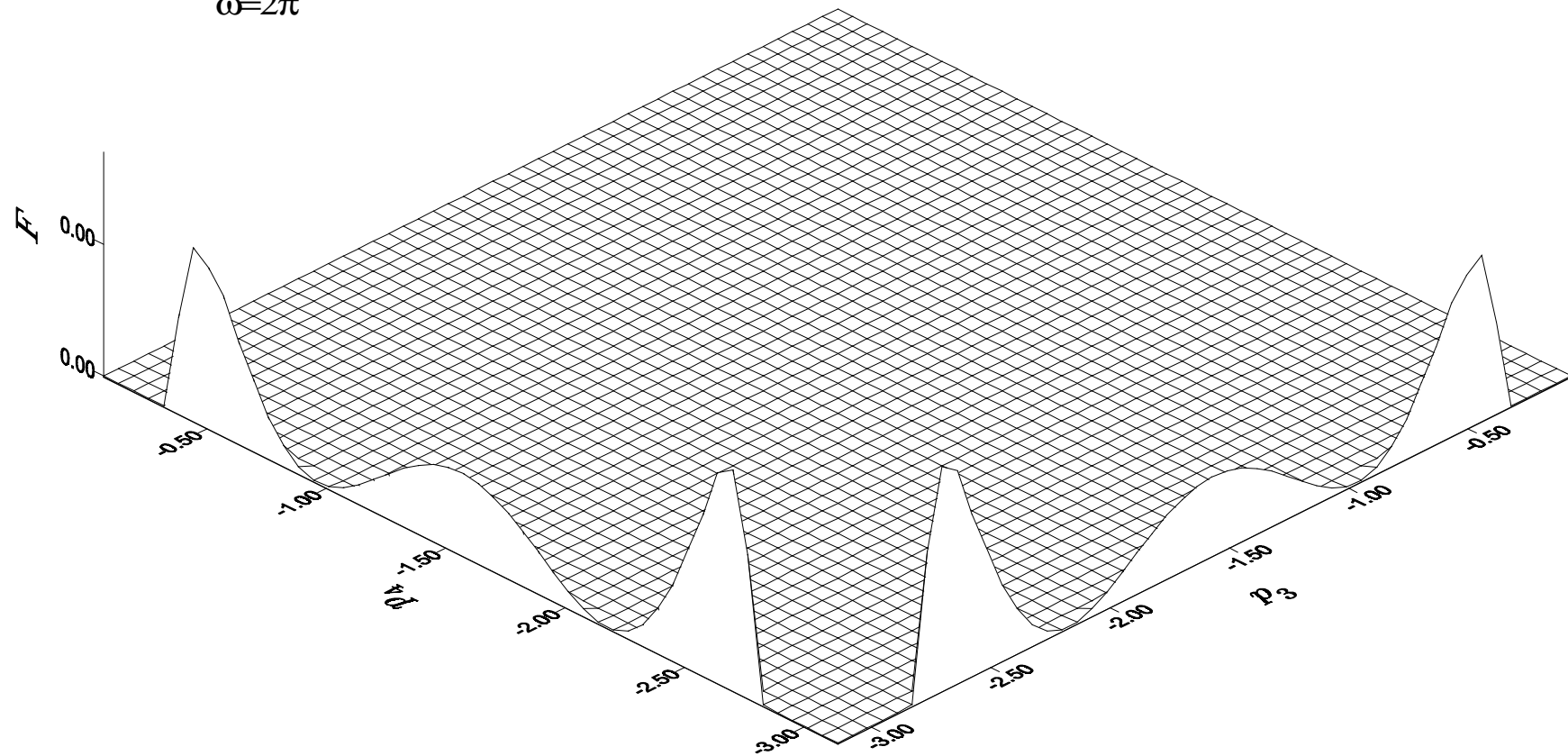


figure 6b

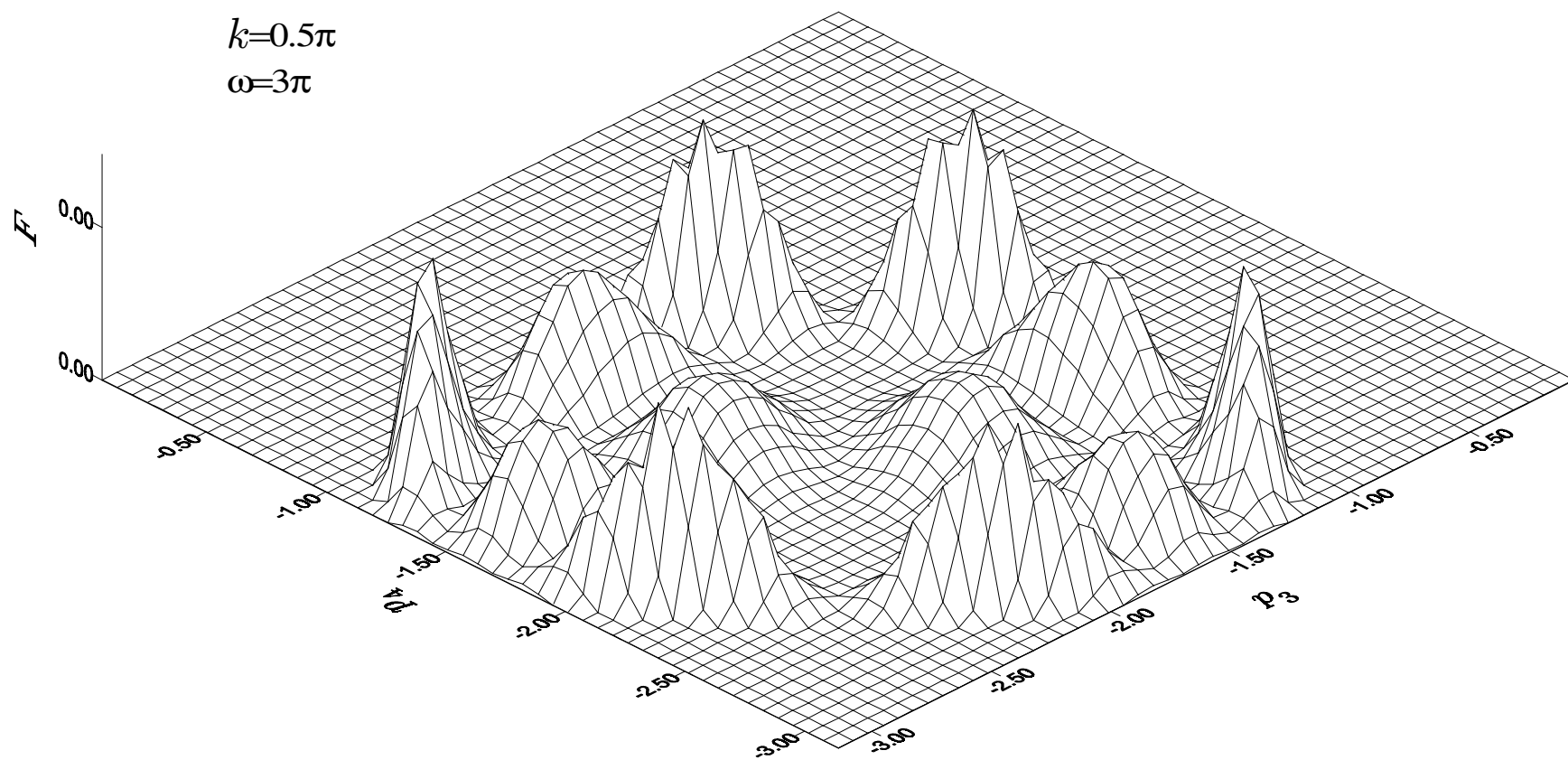


figure 6c

$$\begin{aligned}k &= 0.5\pi \\ \omega &= 3.5\pi\end{aligned}$$

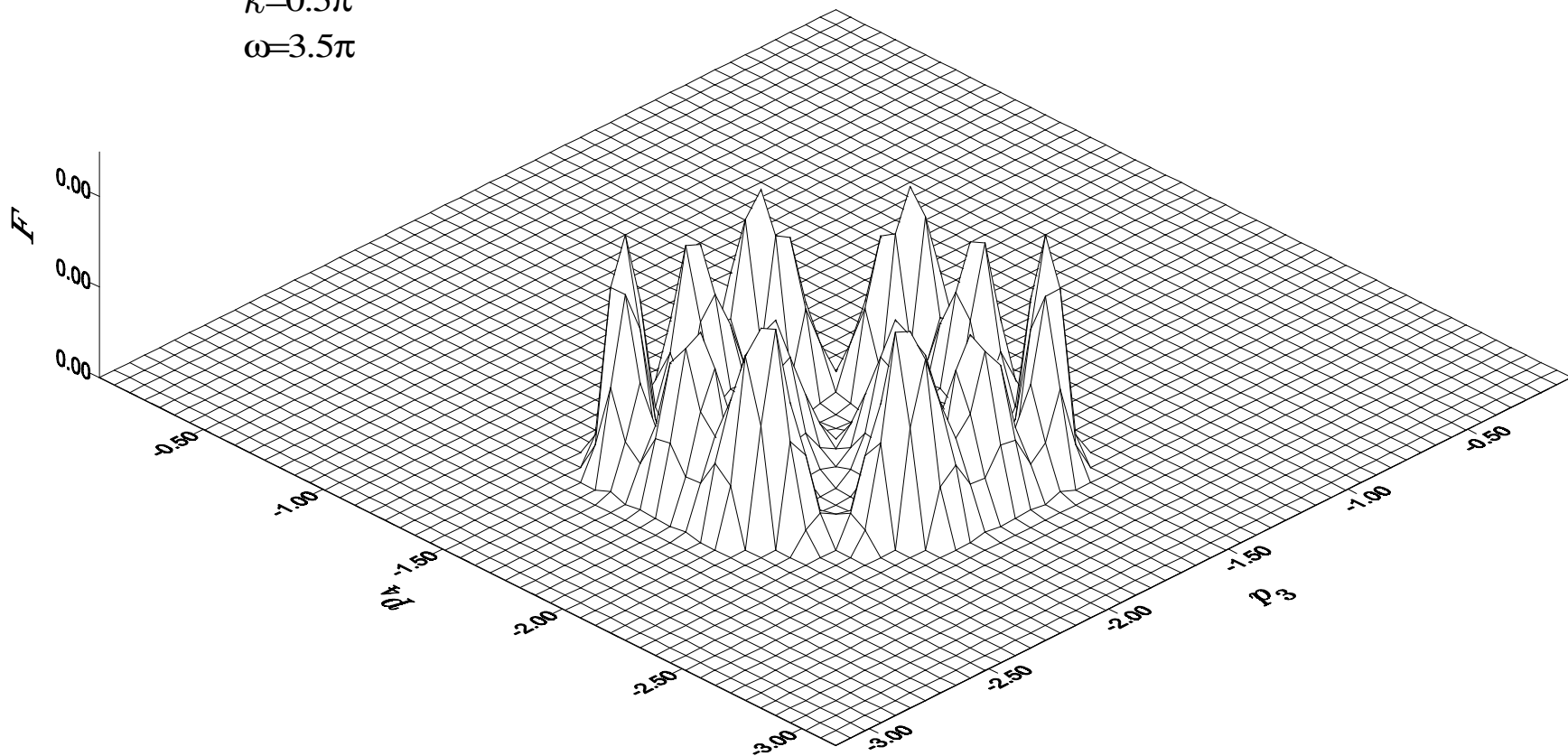


figure 6d

